Observing Nulling of Primordial Correlations via the 21-cm Signal

Shyam Balaji[1,*] H. V. Ragavendra,[2,†] Shiv K. Sethi,[3,4,‡] Joseph Silk,[5,§] and L. Sriramkumar[4,‖]

[1]*Laboratoire de Physique Théorique et Hautes Energies (LPTHE),*
UMR 7589 CNRS and Sorbonne Université, 4 Place Jussieu, F-75252, Paris, France
[2]*Department of Physical Sciences, Indian Institute of Science Education and Research Kolkata, Mohanpur, Nadia 741246, India*
[3]*Raman Research Institute, C. V. Raman Avenue, Sadashivanagar, Bengaluru 560080, India*
[4]*Centre for Strings, Gravitation and Cosmology, Department of Physics, Indian Institute of Technology Madras, Chennai 600036, India*
[5]*Institut d'Astrophysique de Paris, UMR 7095 CNRS & Sorbonne Université, 98 bis boulevard Arago, F-75014 Paris, France*

The 21-cm line emitted by neutral hydrogen (HI) during the Dark Ages carries imprints of pristine primordial correlations. In models of inflation driven by a single, canonical scalar field, we show that a phase of ultra-slow-roll can lead to a *null* in *all* the primordial correlations at a specific wave number $k_{\rm dip}$. We consider scenarios wherein the null in the correlations occurs over wave numbers $1 \lesssim k_{\rm dip} \lesssim 10 \ {\rm Mpc}^{-1}$, and examine the prospects of detecting such a damping in the HI signal due to the nulls at the level of power and bispectra in future observational missions.

Primordial correlations and 21-cm observations.—Cosmic inflation remains the most attractive paradigm for the generation of primordial perturbations. On large scales, e.g., over $10^{-5} \lesssim k \lesssim 1 \ {\rm Mpc}^{-1}$, the primordial scalar power spectrum as generated in some of the popular models of slow roll (SR) inflation is remarkably consistent with the cosmic microwave background (CMB) anisotropies and large-scale structure (for a comprehensive list of inflationary models consistent with the Planck data, see Refs. [1,2]). However, on smaller scales, e.g., $k \gtrsim 1 \ {\rm Mpc}^{-1}$, the constraints on the primordial scalar power spectrum are considerably weaker. Since the discovery of gravitational waves from merging binary black holes, the weaker constraints over small scales have been exploited to examine inflationary models which enhance power on these scales. This leads to significant production of primordial black holes and generation of secondary gravitational waves of observable strengths [3–16].

Often, in single field models of inflation involving the canonical scalar field, a phase of ultra-slow-roll (USR) is invoked to enhance the scalar power on small scales. The first SR parameter ϵ_1 exponentially decreases during such a phase, resulting in large values for the second and higher order SR parameters [4–6,17,18]. Such a departure from SR inflation leads to a peak in the inflationary scalar power spectrum and, generically, one finds that the power spectrum rises as k^4 as it approaches the peak [19–21]. Interestingly, just before the power spectrum rises toward the peak, a sharp drop in power occurs [22] and, if the period of USR inflation is sufficiently long, the scalar power spectrum actually vanishes at a particular wave number, which we denote as $k_{\rm dip}$ [23]. This occurs because of the fact that the mode function describing the curvature perturbation corresponding to the wave number $k_{\rm dip}$ goes to zero at late times toward the end of inflation. It can immediately be shown that all of the higher correlations involving the curvature perturbation will also necessarily vanish at $k_{\rm dip}$. In cases wherein the duration of USR is not sufficiently long, although a null does not arise, a sharp dip in the scalar power spectrum as well as in the higher order correlation functions is still encountered.

Over the scales $1 \lesssim k \lesssim 10 \ {\rm Mpc}^{-1}$, the 21-cm signal of neutral hydrogen (HI) from the Dark Ages carries the signatures of the primordial spectrum (see, e.g., Refs. [24,25]). In contrast to the angular spectra of the CMB, which are a convolution of the primordial spectra and the transfer function of the photons, the features in the primordial power and bispectra leave direct and distinct imprints in the HI signal. Therefore, an inflationary feature such as a null or a sharp dip in the primordial correlations may potentially be observed in HI, if the features occur over the corresponding scales [26]. In this Letter, we consider specific scenarios involving a phase of USR inflation and investigate the effects of a dip on the HI signal at the level of both power and bispectra. If a drop in the scalar power spectrum is to occur over $1 \lesssim k \lesssim 10 \ {\rm Mpc}^{-1}$, we find that the CMB at smaller wave numbers and the spectral distortions at higher wave numbers limit the rise in power on small scales, and hence the extent of the dip. We calculate the corresponding observable signatures on the power and bispectra of the HI signal and discuss the prospects of observing them in future missions, such as a lunar array [27–29]. We also point out challenges that can arise due to Poisson fluctuations (PF) [30,31].

Nulls in inflationary correlations.—We now demonstrate that nulls in the inflationary correlations (i.e., in the scalar power spectrum as well as in higher order correlations) are expected to arise in scenarios involving a phase of

261301-1

USR inflation. Consider a situation wherein a regime of USR inflation is sandwiched between two epochs of SR inflation. Let η denote the conformal time coordinate, and let the two transitions between the three stages occur at the times η_1 and η_2. Also, let the first SR parameter ϵ_1 prior to the first transition be a constant, say $\epsilon_{1i} \lesssim 10^{-2}$, while, during the period of USR, it is given by $\epsilon_1 = \epsilon_{1i}(\eta/\eta_1)^6$. Since $\epsilon_1 \ll 1$ throughout the domains of interest, the Hubble parameter can be considered to be a constant, say, H_I, and hence the scale factor can be assumed to be of the de Sitter form.

Let us focus on the evolution of modes that leave the Hubble radius during the initial SR regime. In the first domain $\eta < \eta_1$, on super-Hubble scales, the mode function characterizing the curvature perturbation in Fourier space, say, f_k^I, can be expressed as

$$f_k^I(\eta) = C_k + \frac{D_k}{2}\eta^2. \tag{1}$$

The constants C_k and D_k can be determined by matching the super-Hubble solutions with the complete solution in the SR regime, and they are found to be $C_k = iH_I/(\sqrt{4k^3\epsilon_{1i}}M_{Pl})$ and $D_k = C_k k^2$. During the USR phase, the modes function, say, f_k^{II}, for modes that are already on super-Hubble scales, can be expressed as

$$f_k^{II}(\eta) = A_k + B_k\left(\frac{1}{\eta^3} - \frac{1}{\eta_1^3}\right). \tag{2}$$

The quantities A_k and B_k can be determined by matching the mode functions and their time derivatives at the transition at η_1 to obtain that $A_k = C_k[1 + (k^2\eta_1^2/2)]$ and $B_k = -D_k\eta_1^5/3$.

When the phase of USR ends, because the wave number of interest is on super-Hubble scales, its amplitude will evidently freeze at its value at the conformal time η_2. We should clarify that such a behavior can also be expected if, for $\eta > \eta_2$, the parameter ϵ_1 begins to grow leading to the termination of inflation. Hence, the power spectrum is determined by the value of f_k^{II} at η_2. Upon setting $f_k^{II}(\eta_2)$ to be zero, we can immediately determine the wave number k_{dip} at which the amplitude of the curvature perturbation vanishes. It is given by

$$k_{dip} = -\frac{1}{\eta_1}\left\{\frac{1}{3}\left[\left(\frac{\eta_1}{\eta_2}\right)^3 - 1\right] - \frac{1}{2}\right\}^{-1/2} \simeq \sqrt{3}k_1 e^{-3\Delta N/2}, \tag{3}$$

where the final expression has been arrived at by assuming that the epoch of USR is adequately long so that $\eta_1/\eta_2 \gg 1$, and we have set $k_1 = -1/\eta_1$ (i.e., the wave number that leaves the Hubble radius at the onset of USR), while ΔN denotes the duration of USR in e folds. The power spectra and all the higher order correlations involve the mode

function f_k evaluated toward the end of inflation. Since the mode function f_k corresponding to the wave number k_{dip} vanishes at late times, any correlation function involving this mode necessarily vanishes as well. However, if the duration of USR is not long enough (in fact, when $e^{\Delta N} \lesssim 5/2$), then the mode function, rather than vanishing, settles down to a very small value at late times. In such cases, a sharp dip is produced rather than a null in the correlation functions, and the relation (3) predicts the location of the dip. Moreover, when the dominant term in the mode function f_k vanishes, the subdominant terms can lead to a small nonzero value at k_{dip}, resulting in a dip as opposed to a null.

Inflationary models, power and bispectra.—To illustrate the nulls or dips that are expected in the correlation functions, we shall consider two models of inflation driven by a single, canonical scalar field that permit a brief period of USR. These models should be treated as illustrative examples of inflationary scenarios generally considered to enhance power on small scales. We shall also briefly discuss a reconstructed scenario which easily allows us to achieve the desired background evolution and a power spectrum that is consistent with the constraints from the CMB on large scales.

The first model we shall consider is a model due to Starobinsky that is described by a linear potential with a sudden change in its slope [32–35]. It is one of the simplest models that leads to a regime of USR and a steplike feature in the scalar power spectrum. The potential describing the Starobinsky model (ST) is given by [32–35]

$$V(\phi) = \begin{cases} V_0 + A_+(\phi - \phi_0) & \text{for } \phi > \phi_0, \\ V_0 + A_-(\phi - \phi_0) & \text{for } \phi < \phi_0, \end{cases} \tag{4}$$

where V_0 sets the overall energy scale. Evidently, A_+ and A_- determine the slopes of the potential on either side of ϕ_0, and the slope is discontinuous at this point. Though there are issues in achieving a natural end to inflation, we consider the model because of its analytical tractability that helps in illustrating arguments related to features induced by USR (in this regard, see Supplemental Material [36]). In the model, the epoch of USR occurs when the field crosses ϕ_0 and the duration of this epoch is determined by the ratio of the slopes of the potential, i.e., A_-/A_+. It can be shown that, in the model, $k_{dip} \simeq \sqrt{3(A_-/A_+)}k_0$, where k_0 is the wave number that leaves the Hubble radius when the field crosses ϕ_0 [32,34,45]. The parameters V_0 and A_+ are constrained by Cosmic Background Explorer (COBE) normalization on the CMB scales (for values of the parameters, see Supplemental Material [36], which includes Refs. [46,47]). The constraints from spectral distortions over the wave numbers $1 < k < 10^4$ Mpc^{-1} limit the extent of enhancement in the power spectrum at small scales [48], and hence the duration of USR. We choose the parameters

A_- and ϕ_0 so that the rise in power on smaller scales is consistent with the Far Infrared Absolute Spectrophotometer (FIRAS) constraints on μ distortions [12]. Also, these parameters are chosen such that the dip in the power spectrum occurs at wave numbers $k \gtrsim 5 \text{ Mpc}^{-1}$ to evade bounds on the matter power spectrum from the Lyman-α data (see, e.g., Refs. [30,49]). For the parameters we work with, we find that $k_{\text{dip}} = 7.6 \text{ Mpc}^{-1}$. We should clarify that, the duration of USR in ST is determined by the ratio of A_-/A_+, which, in turn, determines the height of scalar power at its maximum. Since this amplitude is constrained by μ distortion, it imposes a lower bound on this ratio. Such a bound leads to an inadequate duration of USR, producing a sharp dip, instead of a null in the power spectrum.

The second model we shall consider is an inflationary scenario driven by the Higgs field that is coupled non-minimally to gravitation [14,50–52]. The model is known as critical-Higgs inflation (CH), and the effective potential in this scenario contains a point of inflection, which leads to an epoch of USR thereby enhancing the scalar power over small scales. The potential describing the model can be written as

$$V(\phi) = V_0 \frac{[1 + a(\ln z)^2]z^4}{[1 + c(1 + b \ln z)z^2]^2}, \qquad (5)$$

where $z = \phi/\phi_0$. As in the case of ST, we choose the parameters of the potential so that the power spectrum is consistent with COBE normalization on large scales and with the constraints from spectral distortions on smaller scales. For the values of the parameters we work with (in this regard, see Supplemental Material [36]), we find that a dip in the power spectrum occurs at around $k_{\text{dip}} = 7.6 \text{ Mpc}^{-1}$ and the power reaches its maximum amplitude at around $5.5 \times 10^9 \text{ Mpc}^{-1}$. The μ distortion arising due to this spectrum is found to be about 2.0×10^{-5}, which is within the FIRAS bound [12,48].

It is known that, in single field models of inflation, if the enhancement in power is to be achieved over wave numbers that are close to the CMB scales, there can arise a tension between the value of the scalar spectral index n_S in the model and the constraint on the parameter from the CMB data (for recent discussions, see Refs. [53,54]). In the ST and CH models, the value of n_S at the pivot scale of $k_* = 0.05 \text{ Mpc}^{-1}$ turns out to be 0.9995 and 0.78, respectively, which are well away from the mean value of 0.96 from Planck [55]. One way to circumvent this challenge is to construct inflationary potentials using the desired behavior of $\epsilon_1(N)$ and, interestingly, it can be shown that these reconstructed potentials too contain a point of inflection [10]. In other words, using methods of reconstruction, it is possible to arrive at potentials numerically that are consistent with the CMB data on large scales and lead to a dip
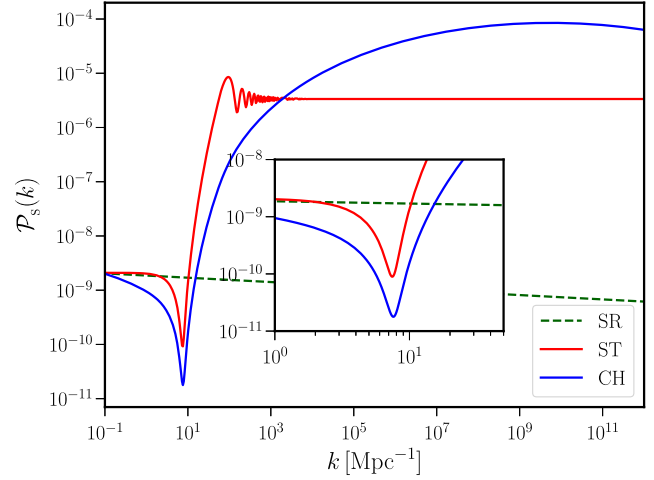
FIG. 1. The inflationary scalar power spectra arising in ST and CH models are illustrated for parameters that are consistent with the constraints on spectral distortions from FIRAS. We have also plotted the nearly scale invariant spectrum that may be obtained from a typical SR model of inflation. The inset highlights the dip in the spectra at $k = 7.6 \text{ Mpc}^{-1}$, and we work with parameters such that the dip occurs over wave numbers where the HI signal is expected to be most sensitive to the primordial power spectrum.

in the power spectrum over $1 \lesssim k \lesssim 10 \text{ Mpc}^{-1}$ (for details, see Supplemental Material [36]).

We find that the features around the dip have the same characteristics in the reconstructed scenario as in the ST and CH models. Therefore, we shall proceed by considering these models and examining their imprints on the 21-cm signal. We evolve the background and compute the scalar power and bispectra numerically (see Supplemental Material [36] for details). In Figs. 1 and 4 (see Appendix A), we have presented the inflationary scalar power and bispectra, i.e., $\mathcal{P}_S(k)$ and $\mathcal{B}_S(\mathbf{k}_1, \mathbf{k}_2, \mathbf{k}_3)$, that arise in the ST and CH models, for the values of the parameters we have worked with.

We note two related points regarding the bispectra. First, in contrast to the power spectrum which is a positive definite quantity, the bispectra can cross zero when departures from slow roll arise. Hence, it may vanish at locations other than k_{dip}. However, these nulls are dependent on the nature of the integrals involved in the computation of the bispectrum and may not be observed at the same locations in the higher order correlations. Therefore, they are not as generic as the dip of interest, which will be located at k_{dip} in the higher order correlations as well. Hence, in models wherein a deviation from slow roll arises due to an epoch of USR, the bispectra are *guaranteed* to exhibit a sharp dip at k_{dip}. Second, note that the power and bispectra in the Starobinsky model rise more sharply than in the Higgs model. This can be attributed to the sharp change in the slope of the potential in the former model [34,56]. Moreover, for the models of interest, the dip in the power spectrum occurs at the linear order of the perturbations.

Though there may arise corrections to the power spectrum due to higher order correlations, we have checked, for instance, that the corrections due to the bispectrum are negligible for the parameters considered.

Imprints on preionization HI signal.—We now turn to discuss the imprints of the inflationary power and bispectra with sharp dips that we have obtained on the 21-cm signal of HI from the Dark Ages. We briefly outline the essential points. In the rest frame of a hydrogen atom, the hyperfine splitting of the ground state causes an energy difference that corresponds to the wavelength of $\lambda = 21.1$ cm. The spin temperature T_S of this line is determined by three processes taking place in the early Universe: emission and absorption of CMB photons with a black body temperature $T_{\rm CMB}$, collisions with atoms, and the mixing of the two levels caused by Ly-α photons (i.e., the Wouthuysen-Field effect). The spin temperature T_S can be expressed in terms of $T_{\rm CMB}$, the gas kinetic temperature T_K, and the color temperature of the Lyman-α photons T_α, as follows [25,57]: $T_S = (T_{\rm CMB} + y_c T_K + y_\alpha T_\alpha)/(1 + y_c + y_\alpha)$. In this expression, y_c and y_α determine the efficacy of the collisions between the hydrogen atoms and of the hydrogen atoms with the Lyman-α photons, respectively. Note that, $y_c \propto n_{\rm HI}$ and $y_\alpha \propto n_\alpha$, where $n_{\rm HI}$ and n_α denote the number density of HI and the Lyman-alpha photons. HI emits or absorbs 21-cm radiation from the CMB depending on whether T_S is greater than or less than $T_{\rm CMB}$. This global temperature difference is observable and can be expressed as [25,58,59]

$$\Delta T_b(z) \simeq 30 \left(1 - \frac{T_{\rm CMB}}{T_S}\right)\left(\frac{1+z}{10}\right)^{1/2}\left(\frac{\Omega_b h^2}{0.022}\right) \text{ mK}. \quad (6)$$

The signal is observable at the frequency of 1420 MHz$/(1 + z)$ at a given redshift z.

Before the onset of the era of cosmic dawn, $y_\alpha = 0$ and the dynamics of T_S is entirely determined by the other two processes. For $z \gtrsim 50$, collisions dominate and hence $T_S \simeq T_K$. As $T_K \simeq T_{\rm CMB}$ for $z \gtrsim 200$, T_S relaxes to $T_{\rm CMB}$ in this redshift range and the observable signal is negligible. At lower redshifts ($z \lesssim 150$), T_K falls adiabatically as $1/a^2$ and, as $T_S \simeq T_K$, HI is observable in absorption. At even smaller redshifts, owing to the dilution of the gas, the collisional coupling becomes progressively weaker and T_S relaxes to $T_{\rm CMB}$, causing the HI signal to diminish.

We have relegated the details of the computation of the power and bispectra of the HI signal to Appendix B. In Fig. 2, we present the HI intensity power spectrum arising in the ST and CH models at the redshifts of $z = 27$ and $z = 50$. In the figure, we have also included the results from a typical SR model, along with the contribution from PF. In Fig. 3, we have illustrated the HI intensity bispectrum arising in the ST and CH models at two redshifts in the
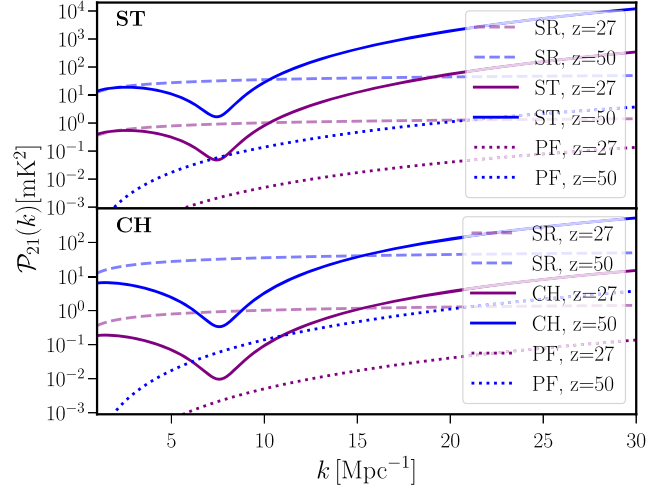
FIG. 2. The HI intensity power spectra arising from the ST and CH models have been plotted at the redshifts of $z = 27$ and $z = 50$. For comparison, we have also presented the HI intensity power spectra arising in a SR scenario leading to a nearly scale invariant, power law primordial scalar power spectrum. We have also included the power spectra due to PF at the corresponding redshifts.

equilateral, squeezed, and flattened limits, along with the contribution from PF.

Our main findings, shown in Figs. 2 and 3, clearly indicate that, in the presence of an epoch of USR, there arises a significant dip in the HI intensity power and bispectra over the scales $1 \lesssim k \lesssim 10$ Mpc^{-1}, when compared to a typical SR scenario. The HI signal arising from the inflationary bispectrum is seen to be smaller than the
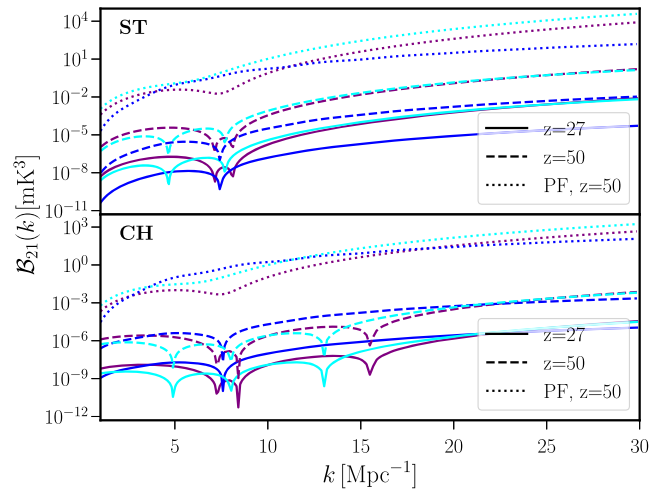
FIG. 3. The HI intensity bispectra arising from the ST and CH models have been presented in the equilateral, squeezed and the flattened limits with the same choice of colors as in Fig. 4. We have focused around $k_{\rm dip}$ and we have set $k_{\rm sq} = k/100$ to arrive at the behavior in the squeezed limit. The associated PF have also been indicated.

contribution from PF by many orders of magnitude. As the Poisson contribution to the bispectrum depends on the HI power spectrum [cf. Eq. (B4)], the detection of this signal would provide further evidence of the presence of a null or a dip in the inflationary power spectrum.

Sensitivity.—We now explore the feasibility of the detection of the HI intensity power spectrum over scales of interest. As can be seen in Fig. 2, our main predictions are over the scales $1 \lesssim k \lesssim 100$ Mpc^{-1}. The signal strength at such scales is of the order of 10–1000 (mK)^2 in the frequency range 25–50 MHz, for the redshift range $z \simeq 25$–50. While the signal at $z \simeq 25$ is accessible to SKA-Low (see, e.g., Ref. [60]), we expect the signal at $z \simeq 50$ to be more pristine (i.e., less contaminated by astrophysical processes close to the era of cosmic dawn) and dominant. Such a signal could be explored by planned lunar missions [27–29]. Under suitable assumptions (for a detailed discussion and methodology, see Supplemental Material [36]), the brightness temperature sensitivity of 1–10 (mK)^2 can be achieved for the scales of interest. A comparison with Fig. 2 immediately suggests that the attainable sensitivity should allow the detection of the dip due to the epoch of USR in the HI power spectrum.

Conclusions.—In models of inflation driven by a single, canonical scalar field, an extended phase of USR leads to a *null* in *all* the primordial correlations at a specific wave number k_{dip}. We have considered scenarios in which the null in the primordial correlations occurs over wave numbers $1 \lesssim k_{\mathrm{dip}} \lesssim 10$ Mpc^{-1}. We show that future experiments should have the sensitivity to detect a damping of power in the HI signal due to the nulls at the level of the power and bispectra.

Appendix A: Inflationary scalar bispectrum.—In this Appendix, we have plotted the bispectra in the equilateral (i.e., when $k_1 = k_2 = k_3$), squeezed (when $\boldsymbol{k}_1 \to 0$ and $\boldsymbol{k}_2 = -\boldsymbol{k}_3 = \boldsymbol{k}$) and flattened (when $k_1 = k_2 = k$ and $k_3 = 2k$) limits. In Fig. 4, we have illustrated the dimensionless quantities such as $k^6 \mathcal{B}_S(k)$ in the equilateral and flattened limits, and $k_1^3 k^3 \mathcal{B}_S(k)$ in the squeezed limit. We find that a dip in the bispectra arises in *all* the limits at the
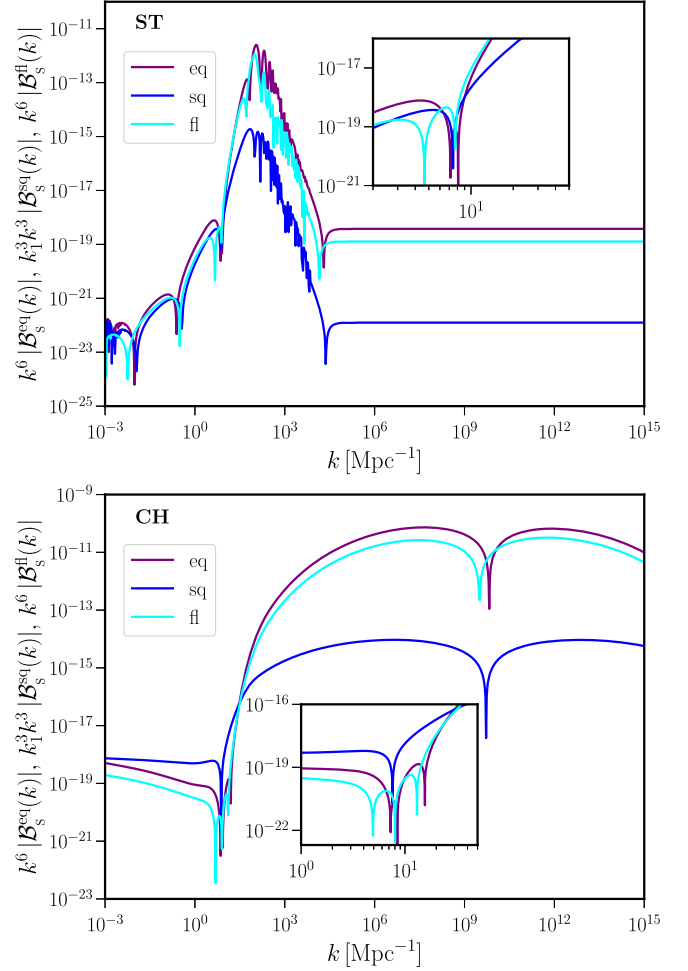
FIG. 4. The scalar bispectra arising in the ST and CH models have been illustrated in the equilateral (eq), squeezed (sq) and flattened (fl) limits. As highlighted in the insets, the bispectra also exhibit a sharp dip at the same location (i.e., at 7.6 Mpc^{-1}) as the power spectra in the previous figure.

same location of the dip (viz. at $k_{\mathrm{dip}} = 7.6$ Mpc^{-1}) in the power spectra.

Appendix B: Computation of power and bispectra of 21-cm signal.—In this Appendix, we provide the details of the computation of power and bispectra of the HI intensity signal in terms of the primordial spectra.

At linear order in the perturbations, the density fluctuations in HI follow the baryonic perturbations. This allows us to express the fluctuating component of the HI signal in the prereionization epoch as $\delta T(\boldsymbol{x}) = \Delta T_b(z) \delta_{\mathrm{HI}}(\boldsymbol{x})$, where $\delta_{\mathrm{HI}}(\boldsymbol{x})$ denotes the inhomogeneities in the density of the neutral gas. We shall ignore the redshift-space distortions in our discussion. At small scales, these perturbations are wiped out due to acoustic damping in the prerecombination era and are regenerated by dark matter potential wells in the postrecombination era. In linear theory, the baryonic perturbations can be expressed in terms of the inflationary

scalar power spectrum as $\mathcal{P}_{HI}(k,z) = T^2(k,z)\mathcal{P}_S(k)$, where $T(k,z)$ is the transfer function for baryons defined such that $T(k,z)$ tends to unity for small k (see, for instance, Ref. [61]). This allows us to write the HI intensity power spectrum at a redshift z in $(\mathrm{mK})^2$ as follows:

$$\mathcal{P}_{21}(k,z) = [\Delta T_b(z)]^2 T^2(k,z)\mathcal{P}_S(k). \qquad (B1)$$

At any redshift, a fraction of baryons, say, f_c, collapse to form halos. The baryons in these halos remain neutral, since for the parameters of interest, the masses of collapsed halos are $\mathcal{O}(10^6 M_\odot)$ and the virial temperature of these halos is less than 1000 K, too small to ionize the gas via collisional processes (we evade the free-free constraints on the excess matter power discussed in Ref. [62]; also see Ref. [63]). The HI intensity power spectrum from PF at a given redshift in $(\mathrm{mK})^2$ is given by (in this context, see, for instance, Ref. [64])

$$\mathcal{P}_{21}^{PF}(k,z) = [f_c \Delta T_b(z)]^2 \frac{k^3}{2\pi^2} \frac{1}{\bar{n}}, \qquad (B2)$$

where $\bar{n}$ is the mean comoving number density of halos. The collapsed fraction f_c and the number density of halos $\bar{n}$ at any redshift can be computed using the Press-Schecheter formalism. For instance, in the CH model, at $z = 50$, $f_c = 0.17$ and $\bar{n} = 18754$ Mpc^{-3}, while at $z = 100$, $f_c = 7 \times 10^{-3}$, and $\bar{n} = 1549$ Mpc^{-3}. At both redshifts, the mass function is dominated by halos of mass $M \lesssim 5 \times 10^5 M_\odot$. At $z = 27$, $\bar{n} = 27638$ Mpc^{-3} and $f_c = 0.45$, with halos of $M \lesssim 2 \times 10^6 M_\odot$ making the most significant contribution to the mass function. We have plotted the spectra $\mathcal{P}_{21}(k,z)$ and $\mathcal{P}_{21}^{PF}(k,z)$ for the ST and CH models in Fig. 2.

Given the scalar bispectrum $\mathcal{B}_S(\boldsymbol{k}_1, \boldsymbol{k}_2, \boldsymbol{k}_3)$ generated during inflation, the HI intensity bispectrum at any redshift can be expressed in units of $(\mathrm{mK})^3$ as

$$\mathcal{B}_{21}(\boldsymbol{k}_1, \boldsymbol{k}_2, \boldsymbol{k}_3, z) = \frac{[\Delta T_b(z)]^3}{2\pi^2} T(k_1, z) T(k_2, z) T(k_3, z)$$
$$\times \frac{k_1^3 k_2^3 k_3^3}{(k_1^3 + k_2^3 + k_3^3)} \mathcal{B}_S(\boldsymbol{k}_1, \boldsymbol{k}_2, \boldsymbol{k}_3). \quad (B3)$$

Also, the bispectrum from PF of discrete sources is given by (see, e.g., Ref. [64])

$$\mathcal{B}_{21}^{PF}(\boldsymbol{k}_1, \boldsymbol{k}_2, \boldsymbol{k}_3, z) = \frac{f_c^3 k_1^3 k_2^3 k_3^3 \Delta T_b(z)}{(k_1^3 + k_2^3 + k_3^3)\bar{n}} \left\{ -\frac{2[\Delta T_b(z)]^2}{\bar{n}} \right.$$
$$\left. + \frac{\mathcal{P}_{21}(k_1)}{k_1^3} + \frac{\mathcal{P}_{21}(k_2)}{k_2^3} + \frac{\mathcal{P}_{21}(k_3)}{k_3^3} \right\}. \quad (B4)$$

We have presented the HI intensity bispectrum at redshifts of $z = 27$ and 50 in Fig. 3 along with the corresponding PF computed at $z = 50$.

*sbalaji@lpthe.jussieu.fr
†ragavendra.pdf@iiserkol.ac.in
‡sethi@rri.res.in
§silk@iap.fr
‖sriram@physics.iitm.ac.in

[1] J. Martin, C. Ringeval, and V. Vennin, Phys. Dark Universe **5–6**, 75 (2014).
[2] J. Martin, C. Ringeval, R. Trotta, and V. Vennin, J. Cosmol. Astropart. Phys. 03 (2014) 039.
[3] M. A. Latif and A. Ferrara, Pub. Astron. Soc. Aust. **33**, e051 (2016).
[4] J. Garcia-Bellido and E. Ruiz Morales, Phys. Dark Universe **18**, 47 (2017).
[5] G. Ballesteros and M. Taoso, Phys. Rev. D **97**, 023501 (2018).
[6] C. Germani and T. Prokopec, Phys. Dark Universe **18**, 6 (2017).
[7] K. Kannike, L. Marzola, M. Raidal, and H. Veermäe, J. Cosmol. Astropart. Phys. 09 (2017) 020.
[8] B. Carr and J. Silk, Mon. Not. R. Astron. Soc. **478**, 3756 (2018).
[9] I. Dalianis, A. Kehagias, and G. Tringas, J. Cosmol. Astropart. Phys. 01 (2019) 037.
[10] H. V. Ragavendra, P. Saha, L. Sriramkumar, and J. Silk, Phys. Rev. D **103**, 083510 (2021).
[11] H. V. Ragavendra, L. Sriramkumar, and J. Silk, J. Cosmol. Astropart. Phys. 05 (2021) 010.
[12] A. D. Gow, C. T. Byrnes, P. S. Cole, and S. Young, J. Cosmol. Astropart. Phys. 02 (2021) 002.
[13] J. Garcia-Bellido, M. Peloso, and C. Unal, J. Cosmol. Astropart. Phys. 12 (2016) 031.
[14] H. V. Ragavendra, Phys. Rev. D **105**, 063533 (2022).
[15] S. Balaji, J. Silk, and Y.-P. Wu, J. Cosmol. Astropart. Phys. 06 (2022) 008.
[16] S. Balaji, G. Domenech, and J. Silk, J. Cosmol. Astropart. Phys. 09 (2022) 016.
[17] N. C. Tsamis and R. P. Woodard, Phys. Rev. D **69**, 084005 (2004).
[18] W. H. Kinney, Phys. Rev. D **72**, 023515 (2005).
[19] C. T. Byrnes, P. S. Cole, and S. P. Patil, J. Cosmol. Astropart. Phys. 06 (2019) 028.
[20] G. Tasinato, Phys. Rev. D **103**, 023535 (2021).
[21] P. S. Cole, A. D. Gow, C. T. Byrnes, and S. P. Patil, arXiv:2204.07573.
[22] O. Özsoy and G. Tasinato, Phys. Rev. D **105**, 023524 (2022).
[23] G. Goswami and T. Souradeep, Phys. Rev. D **83**, 023526 (2011).
[24] M. F. Morales and J. S. B. Wyithe, Annu. Rev. Astron. Astrophys. **48**, 127 (2010).
[25] J. R. Pritchard and A. Loeb, Rep. Prog. Phys. **75**, 086901 (2012).
[26] J. B. Muñoz, E. D. Kovetz, A. Raccanelli, M. Kamionkowski, and J. Silk, J. Cosmol. Astropart. Phys. 05 (2017) 032.
[27] S. Furlanetto et al., arXiv:1903.06212.
[28] P. S. Cole and J. Silk, Mon. Not. R. Astron. Soc. **501**, 2627 (2021).
[29] L. V. E. Koopmans et al., Exper. Astron. **51**, 1641 (2021).

[30] N. Afshordi, P. McDonald, and D. N. Spergel, Astrophys. J. Lett. **594**, L71 (2003).

[31] K. J. Mack and D. H. Wesley, arXiv:0805.1531.

[32] A. A. Starobinsky, Pis'ma Zh. Eksp. Teor. Fiz. **55**, 477 (1992) [JETP Lett. **55**, 489 (1992)].

[33] F. Arroja and M. Sasaki, J. Cosmol. Astropart. Phys. 08 (2012) 012.

[34] J. Martin and L. Sriramkumar, J. Cosmol. Astropart. Phys. 01 (2012) 008.

[35] V. Sreenath and L. Sriramkumar, J. Cosmol. Astropart. Phys. 10 (2014) 021.

[36] See Supplemental Material at http://link.aps.org/supplemental/10.1103/PhysRevLett.129.261301 for details about model parameters, reconstruction and instrumental sensitivities, which includes Refs. [37–44].

[37] J. M. Maldacena, J. High Energy Phys. 05 (2003) 013.

[38] D. Seery and J. E. Lidsey, J. Cosmol. Astropart. Phys. 06 (2005) 003.

[39] X. Chen, Adv. Astron. **2010**, 638979 (2010).

[40] F. Arroja and T. Tanaka, J. Cosmol. Astropart. Phys. 05 (2011) 005.

[41] D. K. Hazra, L. Sriramkumar, and J. Martin, J. Cosmol. Astropart. Phys. 05 (2013) 026.

[42] S. Paul et al., Astrophys. J. **833**, 213 (2016).

[43] R. B. Wayth, S. J. Tingay, C. M. Trott, D. Emrich, M. Johnston-Hollitt, B. McKinley, B. M. Gaensler, A. P. Beardsley, T. Booler, B. Crosse et al., Pub. Astron. Soc. Aust. **35**, e033 (2018).

[44] S. R. Furlanetto, S. P. Oh, and E. Pierpaoli, Phys. Rev. D **74**, 103502 (2006).

[45] H. V. Ragavendra, L. Sriramkumar, and J. Martin (to be published).

[46] J. Martin, L. Sriramkumar, and D. K. Hazra, J. Cosmol. Astropart. Phys. 09 (2014) 039.

[47] H. V. Ragavendra, D. Chowdhury, and L. Sriramkumar, Phys. Rev. D **106**, 043535 (2022).

[48] J. Chluba et al., Exper. Astron. **51**, 1515 (2021).

[49] M. McQuinn, Annu. Rev. Astron. Astrophys. **54**, 313 (2016).

[50] J. M. Ezquiaga, J. Garcia-Bellido, and E. Ruiz Morales, Phys. Lett. B **776**, 345 (2018).

[51] F. Bezrukov, M. Pauly, and J. Rubio, J. Cosmol. Astropart. Phys. 02 (2018) 040.

[52] M. Drees and Y. Xu, Eur. Phys. J. C **81**, 182 (2021).

[53] L. Iacconi, H. Assadullahi, M. Fasiello, and D. Wands, J. Cosmol. Astropart. Phys. 06 (2022) 007.

[54] A. Karam, N. Koivunen, E. Tomberg, V. Vaskonen, and H. Veermäe, arXiv:2205.13540.

[55] N. Aghanim et al. (Planck Collaboration), Astron. Astrophys. **641**, A6 (2020).

[56] A. A. Starobinsky, Phys. Lett. **91B**, 99 (1980).

[57] G. B. Field, Proc. IRE **46**, 240 (1958).

[58] N. Y. Gnedin and P. A. Shaver, Astrophys. J. **608**, 611 (2004).

[59] S. K. Sethi, Mon. Not. R. Astron. Soc. **363**, 818 (2005).

[60] L. V. E. Koopmans et al., Proc. Sci., AASKA14 (**2015**) 001.

[61] S. Dodelson, Modern Cosmology/ Scott Dodelson. Amsterdam (Netherlands) (Academic Press, New York, 2003), pp. XIII and 440, ISBN 0-12-219141-2.

[62] K. T. Abe, T. Minoda, and H. Tashiro, Phys. Rev. D **105**, 063531 (2022).

[63] A. Cattaneo, I. Koutsouridou, E. Tollet, J. Devriendt, and Y. Dubois, Mon. Not. R. Astron. Soc. **497**, 279 (2020).

[64] P. J. E. Peebles, The Large-Scale Structure of the Universe (Princeton University Press, Princeton, New Jersey, 1980).